

# Fundamental Insight and Solvent Dependent Photophysical Properties of Poly(2-Methoxy 5-(2-Ethylhexyloxy)-1,4-Phenylenevinylene) (MEH-PPV)

ISSN: 2576-8840



**\*Corresponding author:** Sangeetha Ashok Kumar, Central Institute of Petrochemicals Engineering and Technology (CIPET), Chennai, TN, India

**Submission:** 📅 December 23, 2021

**Published:** 📅 January 05, 2022

Volume 16 - Issue 3

**How to cite this article:** Sangeetha Ashok Kumar, Jaya Seeli Shankar and Bhuvana K Periyasamy. Fundamental Insight and Solvent Dependent Photophysical Properties of Poly(2-Methoxy 5-(2-Ethylhexyloxy)-1,4-Phenylenevinylene) (MEH-PPV). Res Dev Material Sci. 16(3). RDMS.000886. 2022.  
DOI: [10.31031/RDMS.2022.16.000886](https://doi.org/10.31031/RDMS.2022.16.000886)

**Copyright@** Sangeetha Ashok Kumar. This article is distributed under the terms of the Creative Commons Attribution 4.0 International License, which permits unrestricted use and redistribution provided that the original author and source are credited.

**Sangeetha Ashok Kumar\***, Jaya Seeli Shankar and Bhuvana K Periyasamy

Central Institute of Petrochemicals Engineering and Technology (CIPET), Chennai, India

## Abstract

The Light Emitting Polymer, Poly(2-Methoxy 5-(2-Ethylhexyloxy)-1,4-phenylenevinylene) (MEH-PPV) synthesised via Glich route process with addition of chain stopper to prevent gelation during polymerization was subjected to in-depth characterization. Since solvent interaction is critical in dynamic evolution process of conjugated polymer from solution to film, the present experimental investigation is focused on evaluating the solvent dependent optical properties of MEH-PPV. Photophysical studies indicate that MEH-PPV forms aggregate species with an absorption and luminescence spectra that are distinctly red-shifted from the intrachain exciton in aromatic solvents. The studies revealed better  $\pi$ - $\pi$  interaction in aromatic solvents with the least conformational disorder facilitating improved charge transport, optical and electrical conductivity. While a ridge coiled structure in the case of dissolution in non-aromatic solvent increased the dielectric constant of MEH-PPV. The refractive index ( $\sim 2.6$ ) was not significantly affected by change in solvent polarity. The optical bandgap in aromatic solvent was lesser due to energy migration effect compared to non-aromatic solvent. The dipole-dipole interaction of MEH-PPV in non-aromatic solvent lead to formation of ridged coiled structure with torsional defection which lowered the quantum efficiency of MEH-PPV in non-aromatic solvent (17%) compared to aromatic solvent (24%). The SEM micrographs of thin films prepared from aromatic solvents illustrates smooth surface while surface of thin films from non-aromatic is rough. Additionally, films prepared from aromatic solvents were highly hydrophobic in nature with less porosity. Thus, the effect of non-aromatic solvent to improve the optoelectronic properties of MEH-PPV is though less important than aromatic solvents.

**Keywords:** MEH-PPV; Dielectric constant; Optical conductivity; Electrical conductivity

## Introduction

Enormous researches have been performed in the field Light Emitting Polymers (LEPs) since the discovery of Poly(p-phenylene Vinylene) (PPV) [1]. The LEP represents a novel class of materials, which combine the optoelectronic properties of semiconductors along with the mechanical processability of polymers [2]. LEPs have been potentially used in optoelectronic applications due to their high absorption coefficient and photoluminescence efficiency along with flexibility, less toxicity and low cost [3]. Among the LEPs, the study of PPV as an active material in optoelectronic devices such as Light Emitting Diodes [4,5], Light-Emitting Electrochemical Cell [6], Organic Solar Cells [7] and plastic lasers [8] has been an active area of research. So far, PPV and its derivatives remain the most prominent polymer for PLED applications due to their semiconducting nature, luminescent properties, ease of synthesis and better environmental stability [9,10]. Within the classes of PPVs, poly(2-methoxy 5-(2'-ethylhexyloxy)-1,4-phenylenevinylene) (MEH-PPV) is particularly beneficial for device fabrication as the LUMO level (5eV) matches well with the work function of Indium Tin oxide

(ITO) (~4.8eV) and HOMO level (3eV) is compatible with Physical vapor deposited materials such as Aluminium (~4.1eV) or calcium (~3.5eV) [11]. Moreover, MEH-PPV has asymmetric alkoxy side chains which provides the desired characteristic to be soluble in common organic solvents, allowing the use of thin-film processing techniques such as spin coating, drop-casting and dip coating [12].

The advantageous polymer, MEH-PPV is generally prepared by two novel approaches i) Wessiling route which involves the treatment of dialkylsulfonium salts that yields high molecular weight polymer. ii) Gilch route, employs the treatment of  $\alpha$ - $\alpha'$ -dihalo-p-xylenes with potassium tert-butoxide in the organic solvent [13]. Here, the Gilch route process with slight modification was adopted for the synthesis of MEH-PPV to avoid high temperature processing involved in the Wessiling method.

Since the photophysical characteristics of Light Emitting Polymer (LEP) form the core of optoelectronic applications, this paper invokes a systematic approach to investigate the photophysical properties of MEH-PPV in various solvents. Though there are numerous researches involved in solvent dependent photophysical characterization, the effect of solvent on the optical parameters (Refractive Index, Dielectric Constant and Optical conductivity) and morphology of MEH-PPV thin film is not yet been explored in detail. Thus, this article explains in detail the synthesis procedure, fundamental insight and in-depth characterization of MEH-PPV for PLED applications.

## Experimental

### Materials

MEH-PPV was synthesized by Gilch route process with slight modification [13,14] in three steps [15]. 2-methoxyphenol (PMP) (99% purity), 2-ethylhexyl bromide 95%, sodium hydride (NaH), paraformaldehyde, acetic acid and Hydrobromic acid (HBr 30%) all were purchased from Sigma-Aldrich and used as received. Potassium tert Butoxide (t-BuOK) and benzyl bromide were obtained from TCI chemicals. All the required solvents were obtained from Emplura@ (MERK).

### Methodology

**Synthesis of 1-((2-ethylhexyl)oxy)-4-methoxybenzene (MEHB) - Monomer -I:** To a round bottom flask 10g of PMP and 18.6ml of 2-ethylhexyl bromide were added along with dimethyl formamide (DMF) at room temperature. NaH (0.16mol) was added in batches under continuous stirring at 0 °C, under N<sub>2</sub> atmosphere. After complete addition, the reaction mixture was refluxed at 72

°C for 12 hours in the established N<sub>2</sub> atmosphere. The reaction mixture was cooled to RT followed by extraction of the organic layer with ethyl acetate. The organic mixture was dried over anhydrous magnesium sulphate and purification by distillation yielded ~8.5g of a thick brown solution of MEHB labelled as Monomer -I.

**Synthesis of 1,4 bis(bromomethyl)-2-(2-ethylhexyl)oxy-5-methoxy benzene (MEHDBMB) - Monomer-II:** To a round bottom flask, 15g of MEHB and 4.7 equivalent weight of p-formaldehyde was added. To the reaction vessel, mixture of 5 equivalent weight of 30% HBr and 30mL acetic acid was added dropwise. This reaction mixture was reflux at 80 °C for 48 hours in the N<sub>2</sub> atmosphere. The product was diluted with chloroform followed by extraction with cold water. The organic layer was separated, dried over anhydrous magnesium sulphate and filtered. Later purification by recrystallization through n-Hexane afforded ~11g of pale white color substance which is MEHDBMB labelled as Monomer -II

**Polymerization of 1,4-bis(bromomethyl)-2-((2-ethylhexyl)oxy)-5-methoxybenzene (MEHDBMB):** Polymerization of the MEHDBMD (300gm) was carried out in 30mL THF solution with 2g t-BuOK as the catalyst. To this reaction mixture, 60mg of Benzyl bromide (chain stopper) was added to prevent gelation. The reaction mixture was refluxed at 68 °C for 3 hours in a N<sub>2</sub> atmosphere. The reaction product was precipitated by the addition of 40ml methanol. The precipitate was filtered and washed with distilled water and methanol. Later it was dried in a vacuum oven for 12 hours. It is to be noted that the monomer -2 (MEHDBMD) which was white in color became deep red after polymerization, was associated with the long-conjugated structure of PPV. Thus, the polymerization of MEHDBMB yielded 180mg MEH-PPV. The reaction scheme is represented in Figure 1.

### Physico-chemical characterization

Fourier Transform Infrared (FTIR) spectroscopy and nuclear magnetic resonance (NMR) analysis. Was performed using Nicolet iS5-6700 under attenuated total reflectance (ATR) condition with a wavenumber ranging from 4000cm<sup>-1</sup> to 500cm<sup>-1</sup> and Bruker minispec mq series with deuterated chloroform (CDCl<sub>3</sub>) as the solvent respectively. Scanning electron microscopy (SEM) and energy-dispersive X-ray spectroscopy (EDAX) was performed using JEOL (JSM - 6390 model). The absorbance & emission spectra were obtained through Hitachi, u-2900 spectrophotometer and Horiba, Fluorolog FL-3-11 respectively. The photoluminescence quantum yield ( $\phi_f$ ) of MEH-PPV was estimated through relative measurements in comparison with fluorescein dye ( $\phi_f$ (ref)=0.79).

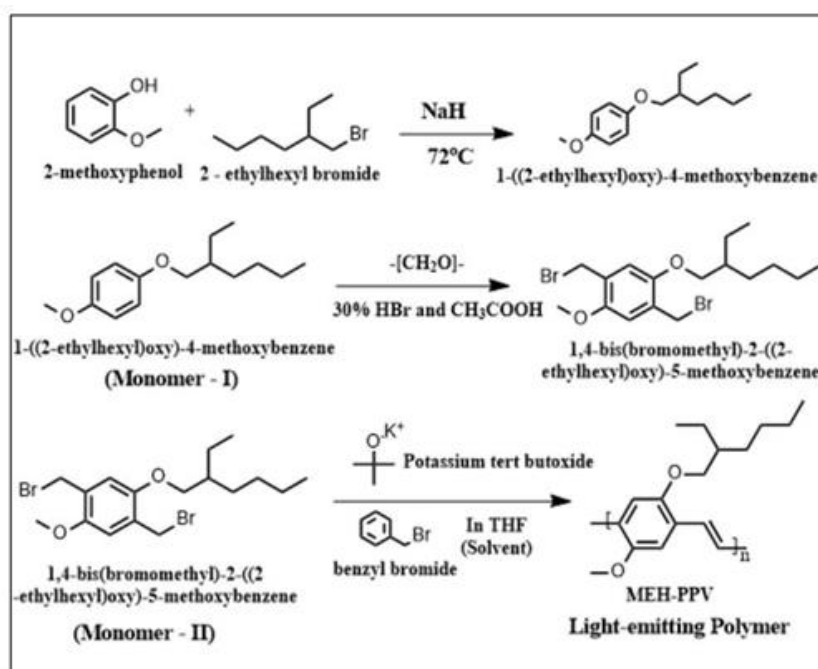


**Figure 1:** Reaction scheme for synthesis of MEH-PPV using gluch route process.

## Results and Discussion

### Functional and structural analysis of MEH-PPV and its monomer

Figure 2 depicts the Fourier Transform Infra-Red spectra of precursor, monomer - I & II and MEH-PPV polymer. It is evident from the FTIR spectrum of MEHB, that after introduction of the 2-ethylhexyloxy side chain, the OH stretching vibration ( $3360\text{cm}^{-1}$ ) on the phenyl ring of PMP (precursor) disappeared, while the intensities for the methyl peak and the new bands of the ethylene group due to introduction of 2-ethylhexyloxy side chain ( $2964\text{cm}^{-1}$ ,  $2949\text{cm}^{-1}$  and  $2824\text{cm}^{-1}$  in MEHB) became stronger. Subsequently,

MEHDBMB prepared by bromomethylation of MEHB. After bromomethylation, Br-C vibrational bands appeared at  $1200\text{cm}^{-1}$  and  $547\text{cm}^{-1}$ . Later polymerization of MEHDBMB, the absorption band of C-Br at  $547\text{cm}^{-1}$  vanished and a new absorption at  $1590\text{cm}^{-1}$  denoting long conjugated double bond appeared. This signifies the occurrence of the polymerization process. On detail examination of FTIR spectrum of MEH-PPV, the bands located at  $863\text{cm}^{-1}$  and  $957\text{cm}^{-1}$  denotes the out-of-plane phenyl CH wag and the trans double bond vinylene C-H wagging respectively. There are three semi-circular stretch modes associated with the phenyl ring denoted by the bands at  $1408\text{cm}^{-1}$ ,  $1509\text{cm}^{-1}$ , and  $1607\text{cm}^{-1}$  [14,16].

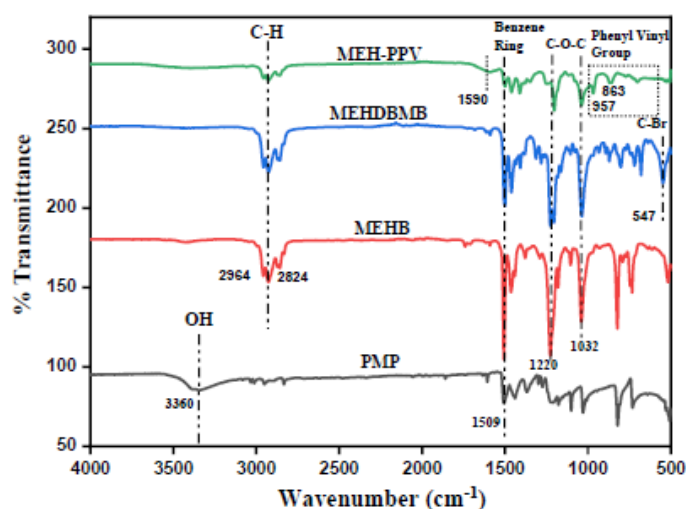


**Figure 2:** FTIR spectra of precursor, monomers and MEH-PPV.

The  $^1\text{H}$  NMR spectra of Monomer I & II and polymer are displayed in Figure 3. It is evident from Figure 3(a) that MEHB contains chemical shift at  $\delta=6.76$  ppm assigned to aromatic protons (benzene ring),  $\delta=0.88$  to  $1.64$  ppm assigned to aliphatic protons (ethylhexyloxy side chain) and  $\delta=3.70$  ppm assigned to methoxy protons. From the NMR spectrum of MEHDBMB (Figure 3(b)) the chemical shifts for bromomethyl on phenyl are assigned at  $\delta=4.57$  ppm. Additionally, NMR denotes benzene ring ( $\delta=6.84$  ppm), methoxy group ( $\delta=3.84$  to  $3.92$  ppm) and 2-ethylhexyloxy group ( $\delta=0.96$  ppm for  $2\text{CH}_3$ ,  $\delta=1.30$ - $1.60$  ppm for methylene and  $\delta=1.80$  for tert-H). Polymerization of MEH-PPV was confirmed through the disappearance of NMR peak for  $-\text{CH}_2\text{-Br}$  at  $\delta=4.57$  ppm and the appearance of new poly (phenylenevinylene) at  $\delta=7.22$  ppm denoting the long-conjugated structure and vinylene group at  $\delta=7.40\sim 7.60$  ppm in Figure 3(c). The results of NMR further support the conclusion drawn from the FTIR studies [14].

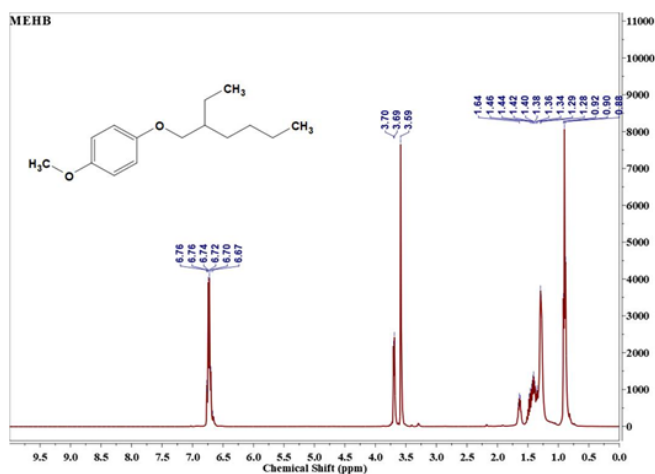


Figure 3a:  $^1\text{H}$  NMR of MEHB (Monomer -1).

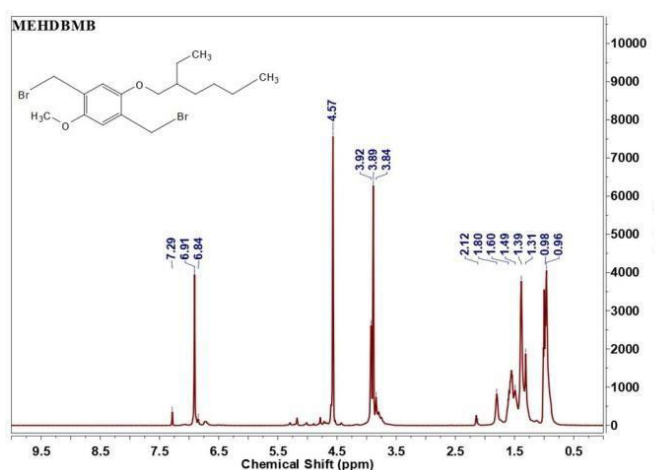


Figure 3b:  $^1\text{H}$  NMR of MEHDBMB (Monomer -2).

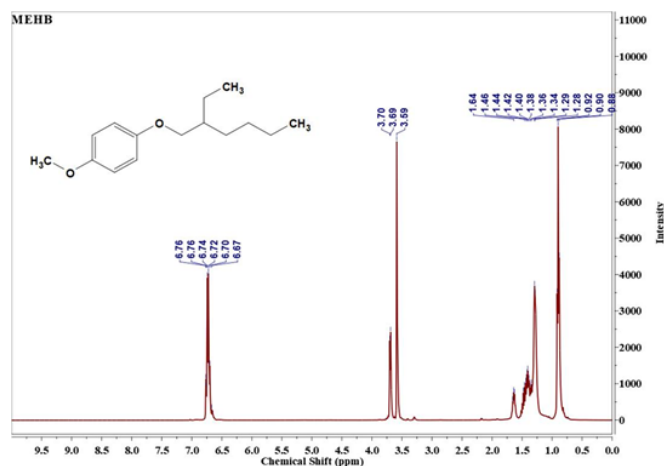


Figure 3c:  $^1\text{H}$  NMR of MEH-PPV.

### Elemental and morphological analysis of MEH-PPV

The morphological and element analysis of MEH-PPV was obtained using SEM and EDAX as shown in Figure 4(a) & 4(b) respectively. This characterization illustrates the highest content of C and O concentration displays the chemical homogeneity of C and O in the prepared samples. The SEM micrographs pertaining to the synthesized polymer powder displays interpenetrating chain like structures which is slightly coiled. The average diameter of polymer chain was estimated to be 230nm. Owing to the interpenetrating nature, the length of the polymer chain was not estimated.

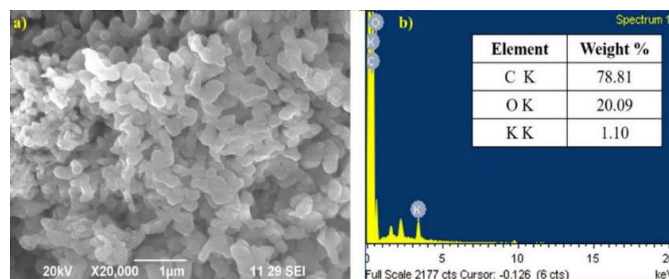


Figure 4: SEM Micrograph and EDAX analysis of MEH-PPV.

### Influence of solvent on the photophysical properties of MEH-PPV

The knowledge of solvation ability is significantly important aspect during multi-layer optoelectronic device fabrications. Nature of solvents affects macromolecular conformation and hence the optoelectronic properties of MEH-PPV. Therefore, the optoelectronic properties of MEH-PPV in various aromatic and non-aromatic solvents was studied. The aromatic solvents (Toluene and Xylene) and non-aromatic solvents (Tetrahydrofuran (THF) and Chloroform) were obtained from Emplura MERK and used as received.

Initially, a stock solution of  $1\text{ mg mL}^{-1}$  concentration was prepared by dissolving prescribe quantity of MEH-PPV in a particular solvent and stirring for it 12 hours in inert atmosphere at  $45\text{ }^{\circ}\text{C}$ .

#### A. Absorbance and steady-state photoluminescence spectroscopy

The normalized absorption and emission spectra of diluted MEH-PPV solutions ( $10^{-2}\text{ mg mL}^{-1}$ ) in toluene, xylene, THF and chloroform are shown in Figure 5. All samples displays a very strong absorption around  $490\text{ nm}$  and a weak absorption at approximately  $330\text{ nm}$ , the former is attributed to the long conjugated double bond connecting with the structures of styryl and stilbenyl groups while the later corresponds to short illuminophores. The presence of twisted points, physical and chemical defects along the conjugated backbone will inhibit the delocalization of electrons throughout the polymer chain. Therefore, a polymeric molecule constitutes of various quasi-localized chromophores with different conjugation lengths. Thus, the distorted polymeric chain with short conjugation length accounted for high-energy photon absorption ( $330\text{ nm}$ ) [17]. The steady state PL spectra produces a dominant peak and a shoulder attribute to monomeric and excimeric states of MEH-PPV.

The emission peak at lower wavelength ( $\sim 550\text{ nm}$ ) arises from single-chain excitons (intrachain excitation). This dominant peak in the emission spectrum is a characteristic of the PPV backbone that arises from the radiative relaxation of excited  $\pi$ -electrons to the ground state. From the literatures, researchers had proven that photoexcitation in conjugated polymers produced mainly by intrachain singlet excitons. However, the peak at longer wavelength ( $\sim 595\text{ nm}$ ) is associated with interchain interactive excimers which are related to aggregation of polymer chains in the solution [18]. The aggregates are characterized by delocalization of the electronic wavefunction among two or more chains in both the ground and excited states. Both absorption spectra and the emission spectra of MEH-PPV in aromatic solvents exhibits bathochromic shift compared to MEH-PPV in non-aromatic solvent because of pronounced aggregation effect exhibited by the polymer in aromatic solvents leading to long conjugation length. Moreover, the spectrum tends to shift to a lower wavelength since the polar solvent (non-aromatic solvents) stabilizes the non-polar ground state of MEH-PPV. This implies that  $\pi^*$  has better stability with an increase in polarity [19].

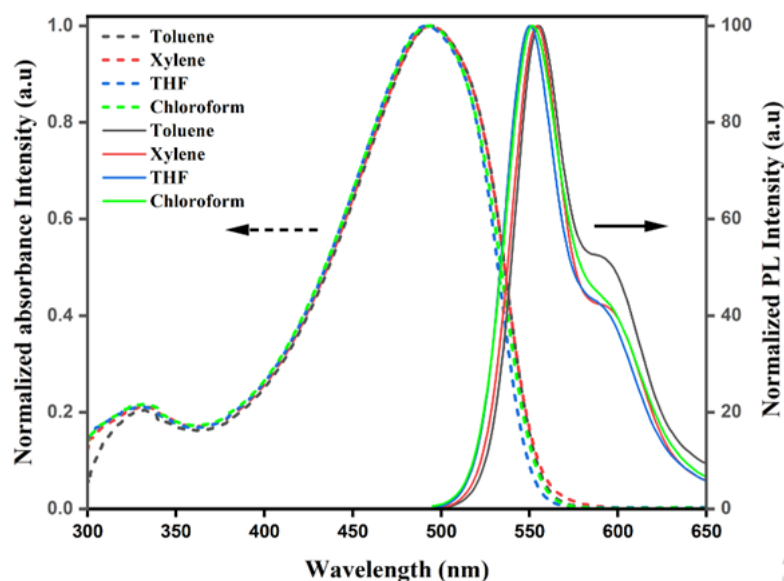


**Figure 5:** Normalized absorbance and emission spectra of MEH-PPV in various solvents.

Optical bandgap ( $E_g$ ), a basic parameter for optoelectronic device development has been evaluated from the absorption spectrum using the Tauc relation:  $(\alpha h\nu)^n = C(h\nu - E_g)$ , where  $C$  is a constant,  $h\nu$  is the photon energy ( $E$ ),  $E_g$  is the optical bandgap of the material and  $n$  is the nature of bandgap ( $n=2$  for MEH-PPV). The  $E_g$  values of MEH-PPV in Toluene, Xylene, THF and chloroform as determined from Tauc plot (given in the Figure 6) are 2.27, 2.28, 2.30 and 2.29 eV

respectively which is in good agreement with the previous reports ( $E_g$  value of MEH-PPV  $\sim 2.3\text{ eV}$ ) [20]. The acceptable reason behind slight decrease  $E_g$  in case of aromatic solvent is that the excitation energy will migrate to longer conjugation lengths before radiative relaxation. This is to be referred to as energy migration through the inhomogeneous density of states.

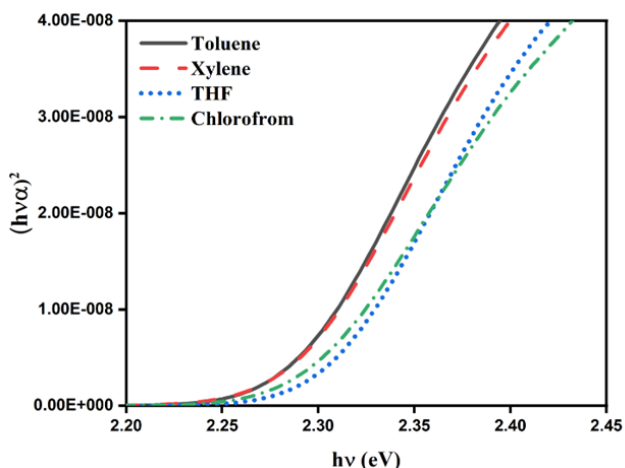


**Figure 6:** Tauc plot.

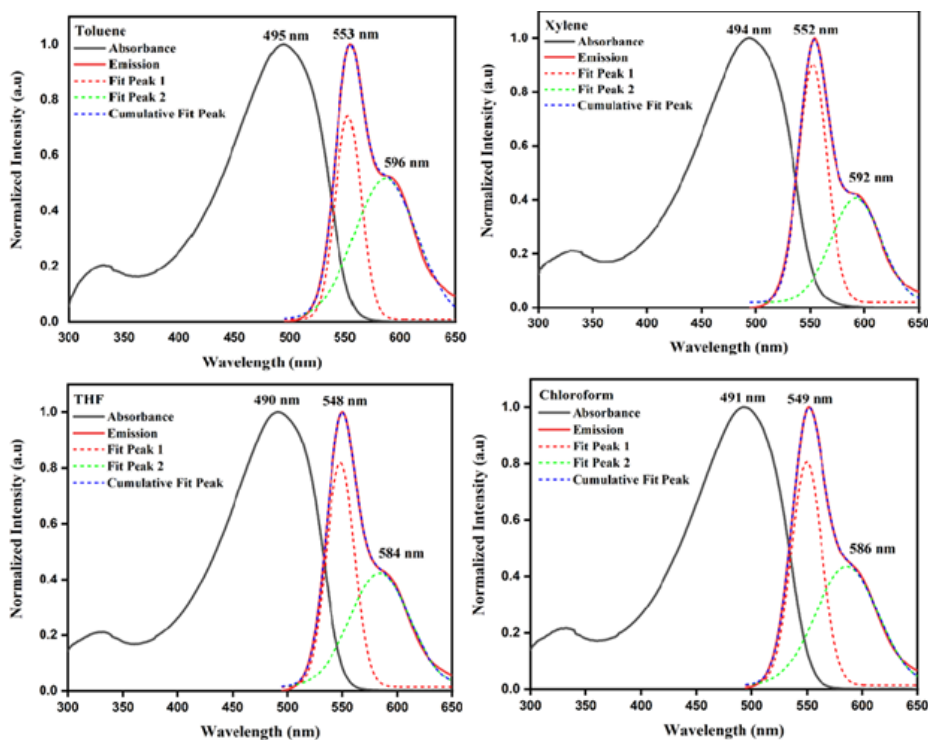


**Figure 7:** Normalized absorbance and fluorescence spectra of MEH-PPV experimental curve (solid curves). The dashed curves displays Gaussian fits of the fluorescence spectra in various solvents.

Huang-Rhys factor ( $S$ ) is obtained by calculating the related strength of the 0-1 peak intensity compared to 0-0 peak intensity:  $S = I_{0-1}/I_{0-0}$  which could be related to the effective conjugation length of the conjugated polymer [22]. According to the empirical function proposed by Yu et al. [23] for the PPV, the relationship between the Huang-Rhys factor  $S$  and the conjugation length  $n$  can be described by equation  $S = a \exp(-n^2/b)$ , where  $a$  and  $b$  are empirically chosen to be 3.2 and 38 respectively [23]. Table 1 reveals a greater conformational disorder exists in non-aromatic solvent than aromatic solvent. This phenomenon is attributed to the solvation ability of various groups in the polymer structure.

## B. Huang-Rhys factor and stroke shift

The conformational disorder of MEH-PPV in solution state is examined by calculating Huang-Rhys factor ( $S$ ). In the emission process, the probability of any 0th vibronic excited state to the  $n$ th

vibronic ground state is given by equation:  $I_{0-n} = \frac{e^{-S} S^n}{n!}$  where  $S$  is the Huang-Rhys factor. Previous studies denote that  $n!$  the Huang-Rhys factor ( $S$ ) correlates directly with the conformational disorder [21]. The ratio between the I0-0 vibronic state and I0-1 vibronic state is estimated by deconvoluting into its vibronic bands using the software origin pro version 8.0 with the spectrum in wavelength scale and fitting the peak profile with gaussian functions. The gaussian fit of the PL spectra is also shown in Figure 7.

Generally, an aromatic solvent has a preferential interaction with the polymer backbone due to  $\pi$ - $\pi$  interaction. Thus MEH-PPV adopt a rigid, open and straight conformation, which favour solute-solvent interaction consequently increasing the conjugation length. While the non-aromatic solvent, preferentially solvates the side chain groups of the polymer. Hence MEH-PPV chains form a much tighter coil as the polymer curls up to minimize favorable interaction there by reducing the conjugation length. Since the lateral groups have several possible special orientations, resulting in partially folded conformations, consequently, conformational disorder increases. On the other hand, the planar conformation in

aromatic solvents imposes greater constraints on the backbone that limit the possible number of conformations [21,24]. Therefore, the limited distributions of conformers always lead to narrower

fluorescence bands ( $FWHM_{\text{toluene}}=27\text{nm}$ ) in aromatic solvents because the number of emissive Franck-Condon (FC) states is reduced [25]; Figure 8.

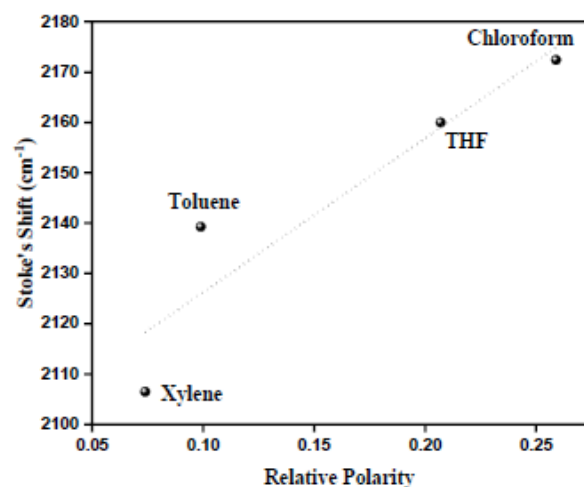


**Figure 8:** Relative polarity of solvent Vs Stoke's Shift.

**Table 1:** Solvent effect on the relative intensity, Huang-Rhys factors and Conjugation length of MEH-PPV.

| Solvent    | I0-0/I0-1 | S (Huang-Rhys Factor) | Conjugation Length (n) | FWHM (nm) |
|------------|-----------|-----------------------|------------------------|-----------|
| Toluene    | 2.75      | 0.363                 | 9.094                  | 27        |
| Xylene     | 2.69      | 0.371                 | 9.048                  | 30        |
| THF        | 2.52      | 0.396                 | 8.910                  | 31        |
| Chloroform | 2.39      | 0.417                 | 8.799                  | 33        |

MEH-PPV has a larger dipole moment in the excited state than in the ground state. The solvation shell that exists around that ground state molecule is inappropriate in the excited state. But due to the Franck-Condon restriction, the solvation shell does not possess ample time for rearrangement. Henceforth after the absorption/excitation process, the solvent dipoles reorients which lowers the energy of the excited state leading to bathochromic shift of emission spectra [26]. This inappropriateness of the shell around the excited state increases with increase in solvent's polarity, which increases the transition energy. Thus, in the case of MEH-PPV dissolved in non-aromatic solvents, the excited state requires rotation of groups on the polymer chain which may display large spectra shift. Thus, the intensity of the emission depends on the excited state. Therefore, the quantum efficiency of MEH-PPV can change based on the rate of radiative decay and the conformational changes [25].

### C. Effect of solvent on optical parameters (refractive index, dielectric constant, optical conductivity and electrical conductivity)

It is well-known that the photophysical behaviour such as shape, intensity, absorbance maxima and optical parameters of a material depends on the nature of the environment and solvent-

solute interaction [27].

Optical constants include the refractive index ( $n$ ), dielectric constant ( $\epsilon$ ), optical conductivity ( $\sigma_{\text{opt}}$ ) and electrical conductivity ( $\sigma_e$ ) are obtained through the following calculation [28,29].

The Refractive index is related to the reflectance  $R$  and extinction coefficient  $k$ .

$$n = \frac{(1+R)}{(1-R)} + \sqrt{\frac{4R}{(1-R)^2} - K^2} \dots\dots\dots\text{eq (1)}$$

where  $k = \frac{\alpha\lambda}{4\pi}$  in which  $\alpha$  is the absorption coefficient given by,  $\alpha = \frac{2.303}{d} A$  where  $d$  is the thickness (path length of 10mm) and  $A$  is the absorbance value.

Dielectric Constant is a complex value ( $\epsilon' + i\epsilon''$ ) comprising of a real and imaginary part.

$$\epsilon' = n^2 - k^2 \dots\dots\dots\text{eq. 2,}$$

$\epsilon'' = 2nk \dots\dots\dots\text{eq. 3,}$  where the imaginary part signifies the loss factor.

Optical Conductivity ( $\sigma_{\text{opt}}$ ) is estimated by

$$\sigma_{opt} = \frac{\alpha nc}{4\pi}$$
 ----- eq. 4 where c is the velocity of light ( $3 \times 10^8$  m/s).

Electrical Conductivity ( $\sigma_e$ ) is determined by

$$\sigma_e = \frac{2\lambda\sigma_{opt}}{\alpha}$$
 ----- eq. 5.

Figure 9 denotes the optical parameters of MEH-PPV in various solvents. Since the nature of the solvent influences the conformational properties of the polymer chain, optical parameters are varied. The refractive index (Figure 9(a)) displays non-linear behaviour and there is no significant variation in the refractive index with the change in solvent [30]. The value of n is  $\sim 2.6$  in all solvents which is close to the reported value [30,31]. The polarizability of any material under the applied electric field is examined by dielectric constant [28]. It can be inferred from Figure 9(b) that MEH-PPV has

the least dielectric constant (6.84) in toluene and highest dielectric constant (6.96) in chloroform. Optical conductivity is a powerful parameter to examine the electronic states in the materials. The optical conductivity of MEH-PPV in toluene ( $6.09 \times 10^8 \text{ S cm}^{-1}$ ) is higher compared to MEH-PPV dissolved in chloroform ( $5.58 \times 10^8 \text{ S cm}^{-1}$ ). Similarly, the electrical conduction of MEH-PPV is enhanced in toluene ( $66 \text{ S cm}^{-1}$ ) compared to non-aromatic solvents. Both MEH-PPV and aromatic solvents possess aromatic ring. Thus, in addition to dipole-dipole interaction, there exists better  $\pi$ - $\pi$  interactions. But non-aromatic solvents provide much different chemical environment where dipole-dipole interaction between the molecule and solvent is prominent. Hence non-aromatic solvents have a stronger interaction with the alkoxy side chain that twist the backbone of MEH-PPV and results in kinked conjugated chains. Rather MEH-PPV displays more planar conformation in aromatic solvents which increases the delocalization of  $\pi$  electrons hence increasing the conductivity of the polymer.

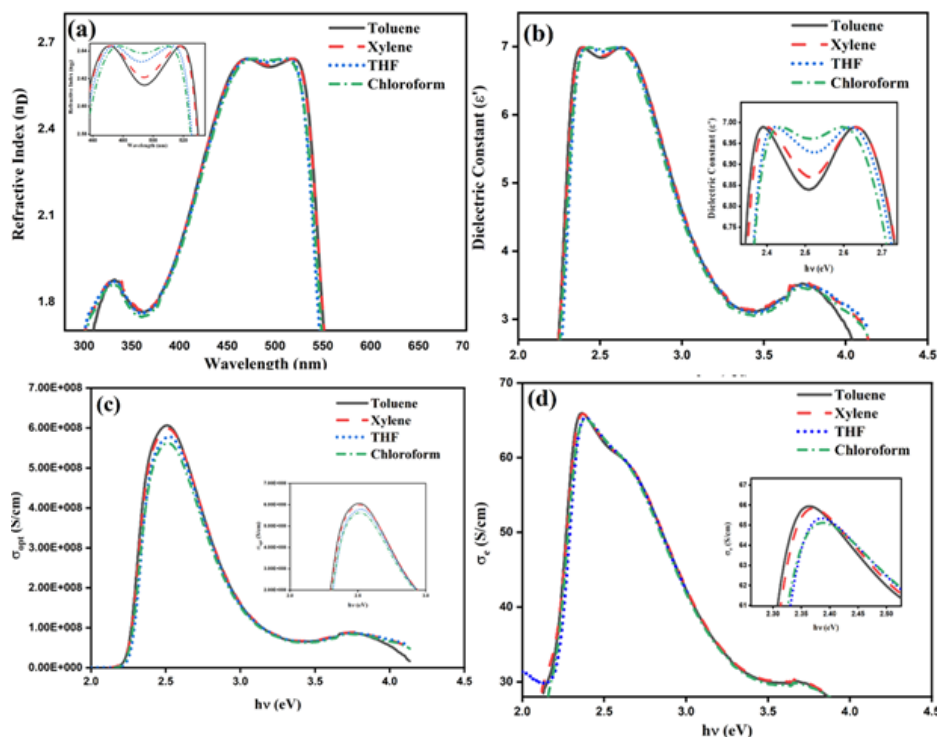


**Figure 9:** Influence of solvent on optical constants measures at  $\lambda$  max (a) Refractive index (b) Dielectric constant ( $\epsilon'$ ) (c) Optical conductance ( $\sigma_{opt}$ ) and (d) Electrical conductance ( $\sigma_e$ ).

#### D. Characteristics of MEH-PPV thin films casted using various solvents

To examine the effect of solvents on emission properties of thin films,  $1 \text{ mg mL}^{-1}$  stock solution was spin coated on 1 in X 1 in cleaned glass substrate at 2000rpm (1 minute) at  $35^\circ \text{C}$  in a  $\text{N}_2$  atmosphere. The coated films were dried at  $40^\circ \text{C}$  for 8 hours for removal of residual solvents. The coated films were subjected to PL analysis

in ambient environment at 490nm excitation. The steady-state PL spectra of MEH-PPV thin films in aromatic and non-aromatic solvents were given in the Figure 10. The emission spectra denoted bathochromic shift for MEH-PPV dissolved in aromatic solvents similar to the observation made in solution state. However, there was trivial decrease PL intensity for aromatic solvents, particular for MEH-PPV in toluene which signifies the quenching owing to aggregation induced effects.

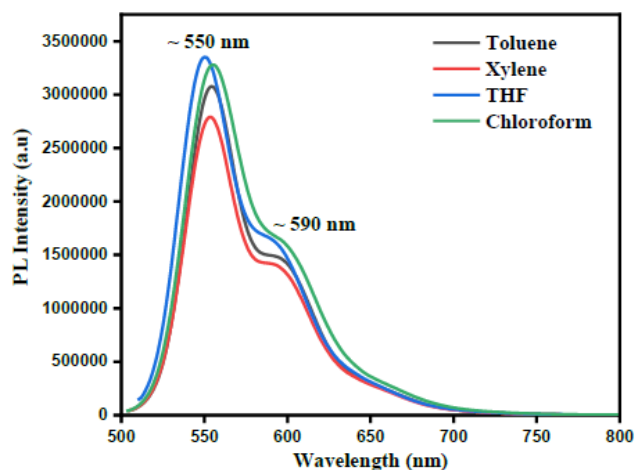


**Figure 10:** PL spectra of MEH-PPV thin films.

Figure 11 illustrates the SEM micrographs of MEH-PPV thin films dissolved in various solvents. The surface of MEH-PPV thin films prepared from non-aromatic solvents (THF and chloroform) are rough and form craters. Because polymer chain in THF and chloroform coil tightly to maximize solvent-side chain interactions while limiting the exposure of aromatic backbone to the solvents.

The thin films prepared from aromatic solvents (toluene and xylene) are smoother because of the preferential interactions between the aromatic backbone and solvents. The open and extend conformation of the polymer chain in aromatic solvents facilitates straight forward overlap of  $\pi$ -electrons with neighbouring chain enable the formation of smooth thin films.

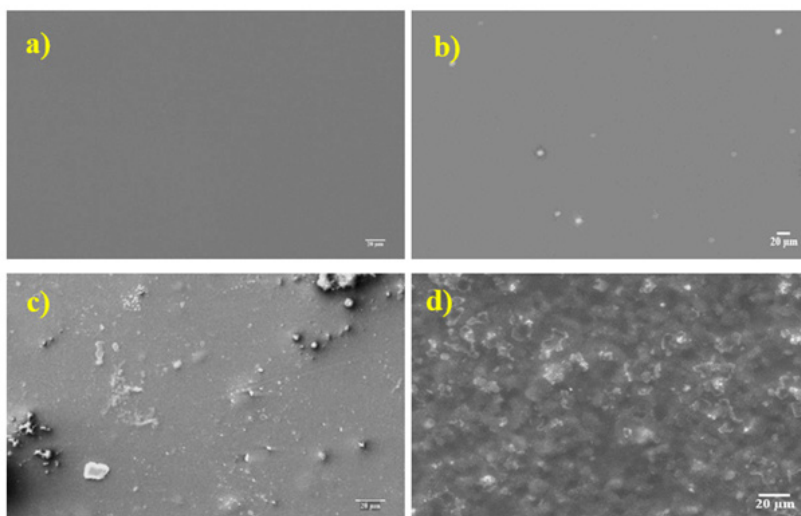


**Figure 11:** SEM Micrographs of MEH-PPV Thin films in (a) toluene (b) xylene (c) THF and (d) chloroform.

To analyze the quality of thin films casted using various solvents, contact angle measurements were performed. Figure 12 displays the contact angle measurements for MEH-PPV thin films. The contact angle in all the case is  $>90^\circ$  indicating the hydrophobic nature of the samples. The higher contact angle for MEH-PPV films casted using toluene indicate compact structure with rigid morphology and a dense film with lesser porosity. Whereas the lower contact angle of MEH-PPV films casted using THF denotes

slight hydrophilic nature, and porosity associated problems owing to the presence of voids which can also be witnessing in the SEM micrographs. The stress/strain eventually leads to defects aiding non-radiative recombination and hence poor charge transport [32]. Thus, thin films prepared using toluene exhibits lower stress and lesser defects are found to be more suitable for optoelectronic applications.

### E. Relative quantum yield measurement for MEH-PPV in various solvents

Fluorescence quantum yield ( $\Phi_f$ ) is the ratio of number of photons emitted to the number of photons absorbed. The relative fluorescence quantum yield measurement was performed for MEH-PPV in comparison with fluorescein. The procedure and formula for estimation of relative quantum efficiency is described elsewhere

[33]. The  $\Phi_f$  of pristine MEH-PPV material in THF and toluene were identified as 16% and 24% respectively. MEH-PPV in THF exhibits a coiled structure which creates torsional defects along the backbone leading to lower photoluminescence (PL) quantum yield. Rather in the case of aromatic solvents (toluene) MEH-PPV exhibits significant  $\pi$ -electron interaction between chromophores on the same chain which is beneficial for efficient charge transfer and higher photoluminescence quantum efficiency.

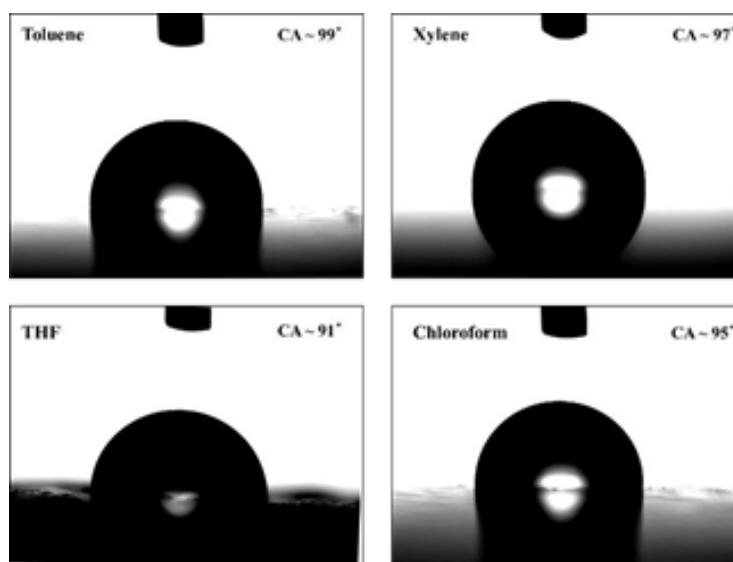


**Figure 12:** Contact angle measurements of MEH-PPV thin films casted using various solvents.

### Conclusion

The light-emitting polymer MEH-PPV was synthesized using Gilch route process with slight modifications. The FTIR and NMR analysis confirms the structures of prepared intermediate products and the polymer. MEH-PPV chains in aromatic solvents are much more extended and open compared to MEH-PPV in non-aromatic, supported by red-shift of absorbance and emission spectra and decrease in Huang-Rhys factor ( $s$ ) and FWHM. This open conformation was due to better  $\pi$ - $\pi$  interaction between MEH-PPV and aromatic solvents which reduced dielectric constant and bandgap of MEH-PPV. The favorable  $\pi$ - $\pi$  interaction in aromatic solvent contributed to improved optical conductivity, electrical conductivity and quantum efficiency. Moreover, MEH-PPV casted from aromatic solvents exhibited smoother surface and higher hydrophobicity. Thus, the improved conductivity nature enabling better charge transport and the smooth surface for MEH-PPV dissolved in aromatic solvent signified that toluene is an apt solvent for MEH-PPV to be used in optoelectronic device fabrications.

### Acknowledgement

The authors are thankful to the Department of Science and Technology (DST) for providing financial support under the

scheme DST – Innovation in Science Pursuit for Inspired Research (INSPIRE), Government of India to carry out this research [DST/INSPIRE Fellowship/2017/IF170799 dated 30.08.2018].

Authors are also grateful to Council of Scientific and Industrial Research (CSIR), Government of India for providing funding to carry out this research. [03(1376)/16/EMR-II dated at 26.10.2017]

The authors are also thankful to Dr. M Sugunalakshmi (Sr. Principal Scientist), Polymer Science & Technology, CSIR-Central Leather Research Institute for her laboratory support.

### References

- Burroughes JH (1990) Light-emitting diodes based on conjugated polymers. *Lett to Nat* 347: 539-541.
- Hassan MU, Liu YC, ul Hasan K, Butt H, Chang JF, et al. (2016) Charge trap assisted high efficiency in new polymer-blend based light emitting diodes. *Nanoenergy* 21: 62-70.
- Saxena KJV, Kumar P (2011) Studies on the fluorescence properties of conjugated polymer poly[2-methoxy-5-(3',7'-dimethyloctyloxy)-1,4-phenylenevinylene] in presence of nitrogen dioxide gas. *Synth Met* 161: 369-372.
- Kim K, Lee DW, Jin J (2000) Electroluminescence properties of poly[2-(2'-ethylhexyloxy)-5-methoxy-1,4-phenylenevinylene]/tris(8-hydroxyquinoline) aluminum two-layer devices. *Synth Met* 114: 49-56.

5. Kwon SH, Paik SY, Yoo JS (2002) Electroluminescent properties of MEH - PPV light-emitting diodes fabricated on the flexible substrate. *Synth Met* 130: 55-60.
6. Pei Q, Yu G, Zhang C, Yang Y, Heeger AJ (1995) Polymer light-emitting electrochemical cells. *Science* 269: 1086-1088.
7. Mahmoud FA, Assem Y, Shehata AB, Motaung DE (2016) Synthesis and characterization of MEH-PPV for solar cell application. *Egypt J Chem* 59(5): 911-933.
8. Masilamani V, Ibnaouf KH, Alsalmi MS, Yassin OA (2007) Laser properties of a conjugate polymer (MEH-PPV) in the liquid - excimeric state. *Laser Phys* 17(12): 1367-1373.
9. Sannasi V, Jeyakumar D (2016) Synthesis and characterization of polyphenylene vinylenes having m -terphenyl group: comparison of their optical properties. *Iran Polym J* 25: 831-840.
10. Ibnaouf KH (2013) Optics & laser technology excimer state of a conjugated polymer ( MEH-PPV ) in thinfilms. *Opt Laser Technol* 48: 401-404.
11. Garcia C (2005) Optical and electrical characteristics of LEDs based on a single organic layer. in 2005 Spanish Conference on Electron Devices, Proceedings.
12. Myers JD, Xue J (2012) Organic semiconductors and their applications in photovoltaic devices. *Polym Rev* 52(1): 1-37.
13. Neef CJ, Ferraris JP (2000) MEH-PPV: Improved synthetic procedure and molecular weight control. *Macromolecules* 33: 2311-2314.
14. Pan J, Chen Z, Xiao Y, Huang W (2000) Synthesis and characterization of fully soluble polyphenylenevinylene. *Chinese J Polym Sci* 18(6): 541-549.
15. O'shea R, Wonga WWH (2020) Simple improvements to Gilch synthesis and molecular weight modulation of MEH-PPV. *Polym Chem*, pp: 1-9.
16. Shankar JS, Kumar SA, Periyasamy BK (2018) Studies on optical characteristics of multicolor emitting MEH-PPV/ZnO hybrid nanocomposite studies on optical characteristics of multicolor emitting MEH-PPV/ZnO Hybrid. *Polym Plast Technol Eng* 58(2): 1-10.
17. Traiphol R, Charoenthai N (2008) Effects of conformational change and segmental aggregation on photoemission of illuminophores in conjugated polymer MEH-PPV: Blue shift versus red shift. *Synth Met* 158: 135-142.
18. Cossello RF, Susman MD, Aramendi PF, Atvars TDZ (2010) Study of solvent-conjugated polymer interactions by polarized spectroscopy. *J Lumin* 130: 415-423.
19. Libration MM, Microwave R, Absorption E, X-ray VFL, Electron A. Spectroscopy techniques and information content.
20. Yahya NZ, Rusop M (2012) Investigation on the optical and surface morphology of conjugated polymer MEH-PPV: ZnO nanocomposite thin films. *J Nanomater* 2012: 0-4.
21. Quan S, Teng F, Xu Z, Qian L (2006) Solvent and concentration effects on fluorescence emission in MEH-PPV solution. *Eur Polym J* 42: 228-233.
22. Ou J (2015) Connection between the conformation and emission properties of poly[2-methoxy-5-(2'-ethyl-hexyloxy)-1,4-phenylene vinylene] single molecules during thermal annealing.pdf. *Appl Phys Lett* 106: 123304 (1-5).
23. Chao C, Chuang K, Chen S (1996) Temperature effect on the electronic spectra of poly ( p-phenylenevinylene ). *Synth Met* 82: 159-166.
24. Traiphol R, Charoenthai N (2008) Solvent-induced photoemissions of high-energy chromophores of conjugated polymer MEH-PPV: role of conformational disorder. *Macromol Res* 16(3): 224-230.
25. Lakowicz JR (1983) Principles of fluorescence spectroscopy.
26. Juris A, Ceroni P, Balzani V (2014) Photochemistry and Photophysics: Concepts, Research, Applications.
27. Transactions CS, Zakerhamidi MS, Ghanadzadeh A, Moghadam M (2012) Solvent effects on the UV / visible absorption spectra of some aminoazobenzene dyes. *Chem Sci Tans* 1(1): 1-8.
28. Gündüz B (2015) Optical properties of poly[2-methoxy-5-(3',7'-dimethyloctyloxy)-1,4-phenylenevinylene] light-emitting polymer solutions\_ effects of molarities and solvents. *Polym Bull* 72: 3241-3267.
29. Sangeetha A, Seeli SJ, Bhuvana KP, Kader MA, Nayak SK (2019) Correlation between calcination temperature and optical parameter of zinc oxide (ZnO) nanoparticles. *J Sol-Gel Sci Technol* 91: 261-272.
30. Tammer M, Monkman AP (2002) Measurement of the anisotropic refractive indices of spin cast thin poly (2-methoxy-5-(2'-ethyl-hexyloxy)-p-phenylenevinylene) (MEH-PPV) Films. *Adv Mater* 14(3): 210-212.
31. Liu M (2017) Holographic polymer-dispersed liquid crystal and a distributed feedback laser with adopted laser dye and a semiconducting polymer film. *Materials (Basel)* 10(509): 1-10.
32. Mittal T, Tiwari S, Mehta A, Tiwari SK, Sharma SN (2017) Comparison of polymeric stabilization of organic / inorganic ( MEH-PPV / TiO 2 ) hybrid composites synthesized via different routes. *Colloid Polym Sci* 295: 1097-1107.
33. Kumar SA, Shankar JS, Periyasamy BK, Nayak SK (2021) Role of defective states in MgO nanoparticles on the photophysical properties and photostability of MEH-PPV/MgO nanocomposite. *Phys Chem Chem Phys* 23(39): 22804-22816.